HHS Public Access

Author manuscript

ACS Sens. Author manuscript; available in PMC 2019 July 27.

Published in final edited form as:

ACS Sens. 2018 July 27; 3(7): 1276–1282. doi:10.1021/acssensors.8b00378.

Thin and Flexible Carbon Nanotube-Based Pressure Sensors with Ultra-wide Sensing Range

Sagar M. Doshi[§,†] and **Erik T. Thostenson**[*,§,†,#]

[§]- Department of Mechanical Engineering, University of Delaware, Newark, DE, USA

[†]- Center for Composite Materials, University of Delaware, Newark, DE, USA

[#]- Department of Materials Science and Engineering, University of Delaware, Newark, DE, USA

Abstract

A scalable electrophoretic deposition (EPD) approach is used to create novel thin, flexible and lightweight carbon nanotube-based textile pressure sensors. The pressure sensors can be produced using an extensive variety of natural and synthetic fibers. These piezoresistive sensors are sensitive to pressures ranging from the tactile range (< 10 kPa), in the body weight range (~ 500 kPa), and very high pressures (~40 MPa). The EPD technique enables the creation of a uniform carbon nanotube based nanocomposite coating, in the range of 250–750 nm thick, of polyethyleneimine (PEI) functionalized carbon nanotubes on non-conductive fibers. In this work, non-woven aramid fibers are coated by EPD onto a backing electrode followed by film formation onto the fibers creating a conductive network. The electrically conductive nanocomposite coating is firmly bonded to the fiber surface and shows piezoresistive electrical/mechanical coupling. The pressure sensor displays a large in-plane change in electrical conductivity with applied out-of-plane pressure. In-plane conductivity change results from fiber/fiber contact as well as the formation of a sponge-like piezoresistive nanocomposite "interphase" between the fibers. The resilience of the nanocomposite interphase enables sensing of high pressures without permanent changes to the sensor response, showing high repeatability.

Graphical Abstract

[*] thosten@udel.edu.

ASSOCIATED CONTENT

Supporting Information

The Supporting Information is available free of charge on the ACS Publications website.

Scanning electron micrographs of EPD PEI-CNT specimen (PDF)

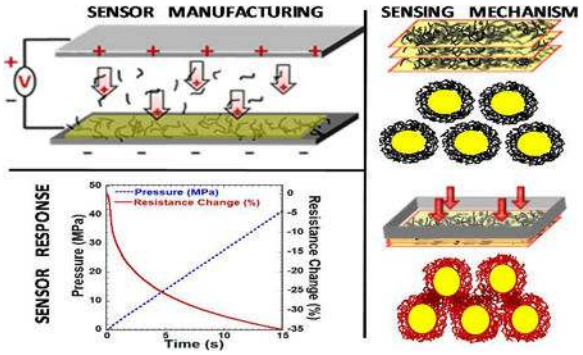

Carbon nanotubes (CNT) functionalized with polyethyleneimine (PEI) are deposited on aramid fibers using an innovative and scalable electrophoretic deposition (EPD) method. The PEI-CNT forms an electrically conductive and mechanically resilient nanocomposite coating, which enables piezoresistive pressure sensing in tactile as well as high pressure range with potential applications in smart textiles and wearable sensors for humans and e skins for robots.

Keywords

Carbon nanotubes; nanocomposites; piezoresistivity; electrophoretic deposition; smart textiles; tactile pressure sensor

Increasingly, there is interest in the development of highly flexible and sensitive pressure sensors that can detect a wide range of pressures. These sensors have a vast potential to be used for applications where surface complexity, thickness limitations and sensitivity are critical, such as electronic skin. These sensors could potentially stimulate applications in the fields of soft robotics, human-machine interfacing, electronic gloves,[1] touch detection, biomedical devices and prostheses, and human motion analysis. While conventional pressure sensors were bulky and mostly based on diaphragms and hydraulics, in recent years the sensing mechanisms for pressure sensors have expanded to include capacitive sensing,[2–5] piezoelectric sensing,[6] triboelectric sensing,[7] and piezoresistive sensing.[8]

The electrical resistance of a piezoresistive pressure sensor changes as a result of the applied pressure. Commonly used piezoresistive sensors are elastomer-based conductive composites and are popular due to low cost, stretchability, flexibility, and ease of fabrication. Frequently used additives as the conductive phase in elastomers include carbon black, metal powders, carbon fiber and carbon nanotubes. However, these elastomer-based pressure sensors are unstable and incapable of measuring a wide range of pressures. The performance of the sensors is limited by the mechanical properties of the elastomer, and the sensing response is often slow and delayed due to the elastomer viscoelastic properties. The quantity of conductive additives that can be added to an elastomer is also limited by the increasing viscosity of the polymer.

Pressure sensors have been fabricated using a variety of unique active elements such as ultrathin gold wires, ZnO nanowires,[9] silver nanowires,[10] organic field effect transistors, graphene, gold nanoparticles, silver nanoparticles,[11] liquid based active materials[12] and carbon

nanotubes.[7–9] Recently, novel microstructures have been used, such as microcrack-designed carbon black polyurethane (PU) foam, micropyramid arrays, microstructured rubber dielectric layers, hollow sphere microstructures produced from polypyrrole hydrogel, interlocking arrays of platinum coated polymeric nanofibers, fractured microstructure design of graphene-PU foam, laser scribed graphene films patterned as v-shaped gratings and reverse-micelle-induced porous rubber. Large scale implementation of these pressure sensors is limited because of factors such as complex and non-scalable fabrication processes, use of expensive materials such as gold/silver and low range of pressure sensing ability. As a result, there exists a critical need for cost effective, pressure sensing materials with large area coverage and a wide range of pressure sensing capability. Commercially-available multi-walled carbon nanotubes are available at relatively low cost and they can be bent through large angles and strains without mechanical failure and can resist failure under repeated bending.[9] Researchers have also reported reversible, periodic buckling of nanotubes consistent with calculations extrapolated from continuum mechanics.[8–10]

Here, we demonstrate a simple, light-weight, breathable and conformable textile pressure sensor able to detect pressures in the gentle touch range as well as very high pressures. A highly efficient and scalable electrophoretic deposition (EPD) process is used to deposit multi-walled carbon nanotubes under an electric field from a water based dispersion at room temperature. The process is based on the mobility of the carbon nanotube under an applied electric field where the surface of the nanotube is functionalized with the dendritic polyelectrolyte polyethyleneimine (PEI). The PEI protonates with the addition of a mild acid and develops a positive surface charge that stabilizes the dispersion and enables cathodic deposition. Placing non-conductive fibers in direct contact with a metallic electrode enables carbon nanotubes to deposit under a direct current (DC) electric field and create uniform, dense films of carbon nanotubes on the surfaces of the fibers. Experimental observations show that the nanotubes deposit first on the electrode and conductive nanotube films then grow over the fibers as an extension of the electrode. Figure 1(a) shows a schematic diagram of the EPD process onto non-conductive fibers.

The amine groups in the PEI form covalent bonds with the oxide groups on the nanotube surface as well as functional groups on the surfaces of fibers.[10–12] The PEI functionalization, approximately 25% by weight, acts as the polymer matrix and creates a porous, flexible, and electrically conductive nanocomposite film on the fiber surface. Figure 1(b) shows electron micrographs of the as-deposited films with PEI functionalized carbon nanotubes onto both wool (left) and aramid (right) fibers, showing a highly uniform, dense coating on the fiber surfaces. The wool fibers have a scale like cuticle structure which is still visible in the coated fibers, and the aramid fibers, cross sectioned with a focused ion beam (FIB), show the uniformity of the coating. As illustrated in Figure 1(c) a piezoresistive nanocomposite formed on the fiber surface results in an in plane change in electrical resistance that is likely from (1) formation of distributed fiber-fiber electrical contacts in the fabric under compression and (2) local piezoresistive response due to the nanocomposite “sensor interphase” – where fiber-fiber contact resistance changes due to local compressive deformation in the nanocomposite coating. The electrical resistance of the sensors in this study is in the range of 5 15 kΩ under no load condition. Figure 1(d) shows the sensitivity of the textile based nanocomposite sensor under pressures in the tactile range (0.0025 – 0.0525

MPa) while Figure 1(e) shows the remarkable sensing capability at pressures up to 40 MPa. This ultra wide range of pressure sensing from 0.0025 MPa to 40 MPa is better than any previously reported data as reviewed by Tian et al.[33] The gauge factor, defined as the slope of the resistance change vs. pressure graph was calculated to be ~ 0.05 MPa^{1}. The sensor response is quite linear at low pressures but becomes nonlinear at higher pressures. This nonlinear response is likely a consequence of the two different mechanisms that influence the in plane electrical response under pressure. The formation of fiber-fiber contacts initially dominates the overall electrical response due to the compressibility of the fabric at low pressures. At higher pressures, the electrically conductive network of nanotubes on the surface of the aramid fibers is compressed. This compression results in a continued decrease in resistance due to the piezoresistive response of the compliant sensor interphase. The piezoresistive response of the carbon nanotube interphase is due to the nanotube-nanotube tunneling resistance within the film. The electrically percolating network of nanotubes on the surface of the fibers changes due to local compression. The compressive stress in the film at the fiber crossover results in a local decrease in the film electrical conductivity. As a result, the resistance at the fiber-fiber contacts decreases with continuously applied pressure.

To further examine the sensing response and the resulting mechanism of sensing, three sets of sensors are compared: (1) aramid fibers coated using EPD with PEI-functionalized carbon nanotubes (EPD PEI-CNT), (2) aramid fibers coated with a commercially available carbon nanotube dispersion/sizing (dip-coating) and (3) a similar non-woven veil composed of conductive carbon fibers (carbon fiber). The EPD coated fibers show much better performance and repeatability while the other sensors show permanent damage at relatively low pressures. Figure 2(a) shows the sensing response of the three sensors at a linearly applied pressure up to 40 MPa followed by releasing of the pressure and Figure 2(b) shows the pressure resistance response for the first 3.5 seconds of Figure 2(a). For all sensors, the resistance decreased until an applied pressure of 2 MPa. For both the carbon fiber and dip-coated sensors, the in plane resistance shows a sharp transition near 2 MPa, as shown in Figure 2(b), followed by increased resistance. Resistance continues to increase in these sensors during both increasing pressure and during unloading where the pressure is decreasing. The increase in resistance despite increasing pressure and a higher number of fiber-fiber contact points is likely due to the physical damage to the sensor. Upon unloading, the carbon fiber and dip-coated sensors show permanent increases in resistance of 246% and 28%, respectively. On the other hand, for the EPD PEI-CNT sensor, a steady decrease in resistance with increasing pressure is observed followed by an increase in resistance during unloading. In contrast to the other two sensors which show large increases in resistance upon unloading, the resistance of the EPD PEI-CNT sensor decreases slightly. To analyze this permanent resistance change, all three sensors were tested under progressively increasing cyclic load. Figure 2(c) shows the permanent resistance change of each sensor with increasing peak pressure. Both the carbon fiber and dip coated sensors show increases in permanent resistance change at higher peak pressures. For the EPD PEI-CNT specimen there is slight decrease in electrical resistance with increasing peak load.

Figure 2(d) shows the morphology of the different sensors before and after loading to 40 MPa. For all sensors before loading the open structure of the random fiber veil is observed. For carbon fiber, the fibers fracture during the loading cycle, likely due to localized bending

at fiber-fiber contact points. Naito *et al.* tested single carbon fibers under transverse compression and observed a brittle failure mode and the specimen fracturing into smaller pieces. Figure 3(a) shows the brittle fracture of the carbon fiber due to local bending at a fiber-fiber contact. The breakage of these long, continuous fibers is likely the cause of the increase in electrical resistance near 2 MPa under the applied pressure and the subsequent large permanent resistance change after unloading. The micrographs of dip-coating specimen in Figure 2(d) show overall compaction of the fabric structure after loading. Small debris marked by red boxes in the micrograph is likely from the damage caused to the sensor during loading. Figure 3(b) shows that there is localized debonding of the carbon nanotube coating after compression. As with the carbon fibers this fiber-fiber contact damage is likely the reason for the increase of electrical resistance near 2 MPa and the overall permanent resistance change after loading. For the EPD PEI-CNT specimen, there is no obvious damage to the sensor after loading and the overall fabric structure is not as highly compressed as the dip-coating structure. Figure 3(c) shows localized deformation and flattening of the fibers in the region of fiber-fiber contact. There is no debonding or cracking observed in the PEI-CNT coating, unlike the dip coated fabric. The strong bonding of carbon nanotube film to the aramid fiber may further prevent fiber damage and breakage under local stresses. The slight decrease in electrical resistance upon unloading of the PEI-CNT sensors is likely due to this local flattening of the fiber and larger fiber/fiber contact area.

The EPD PEI-CNT sensor is tested under progressively increasing pressures up to 40 MPa. With each cycle with increasing pressure, a permanent decrease in resistance is observed (Figure 3(d)), possibly due to compression and consolidation of the PEI-CNT and due to increase in fiber fiber contact area due to flattening of the fibers as seen in Figure 3(c). After loading the sensor to a peak load there is no permanent electrical resistance change below that peak load threshold for re-loading. The initial pre-load results in the localized deformation at the fiber-fiber contacts. After initial pre-loading of the sensors, they have been loaded cyclically for 550 cycles from 0 to 5.2 MPa and exhibit a highly repeatable sensing response for all cycles, without any permanent resistance change. The change in resistance for each cycle is about 16% at 5.2 MPa and is consistent throughout the test; Figure 3(e) shows the first 5 and the last 5 cycles. The carbon nanotubes deposited on the aramid fibers are remarkably resilient and exhibit high structural flexibility. These properties of carbon nanotubes along with a robust bonding to aramid fibers due to PEI functionalization enable a repeatable piezoresistive response when the pressure sensor is loaded multiple times.

The ultra-wide sensing range of the carbon nanotube based textile pressure sensors was demonstrated with real-life examples as shown in Figure 4 which shows the ability to detect extremely low pressures in tactile range (Figure 4(a)), body weight (Figure 4(b)) and very high pressures due to the weight of the forklift (Figure 4(c)). When pressure is applied, the resistance decreases and upon removal of pressure, the resistance comes back to its original state and no permanent change in resistance is observed. The change in resistance due to the finger pressure is about 1% and approximately 12% due to the body weight. When a forklift is driven over the sensor, we see a resistance change of over 25%. From these results, the carbon nanotube based pressure sensors exhibited sufficient potential for a variety of applications requiring a wide range of pressure sensing capability. The resistance response is

real time, without any noticeable time lag. This enables applications in the field where pressure changes rapidly, such as analyzing human gait during walking/running by integrating the sensor with footwear. The slight overshoot of the resistance observed upon removal of the pressure is likely a consequence of the sensor adhering slightly while the contacting surface is lifted off.

In conclusion, a thin, light-weight and flexible pressure sensor has been demonstrated by coating a non-woven aramid fabric with PEI functionalized carbon nanotubes using a novel EPD method. The sensor has an extremely versatile range of pressure measurement and can detect low pressures in the tactile range (<10 kPa) to object handling and maneuvering (10–100 kPa) and very high pressures (~40 MPa). The robustness and the repeatability of the sensor was established and real life examples demonstrated. The innovative and scalable EPD processing method to create a resilient PEI-CNT nanocomposite coating enables pressure sensing in a wide range of pressures without permanent damage to the sensor. We envision that this textile based flexible pressure sensor has potential applications ranging from the creation of smart textiles and clothing that can be used for human motion analysis and biomedical prosthesis to e-skins for robots enabling them to sense touch as well as high pressures for object maneuvering and manipulation.

METHODS

Materials and Processing:

Commercially available multi-walled carbon nanotubes grown using chemical vapor deposition (CM 95, Hanwha Nanotech) were dispersed in ultra-pure water using an ultrasonication and ozonolysis approach as described by An *et al.* Two grams of carbon nanotubes are first added to 2 liters of ultra-pure water and mixed with a magnetic stir bar. The mixture is then cooled to 5°C in a water bath and a peristaltic pump (Model MU D01, Major Science) is used to circulate the mixture through an ultrasonic liquid processor with a 12.7 mm diameter horn (Sonicator 3000, Misonix) equipped with a continuous flow cell (800B Flocell, Qsonica) operating at 60 W in a duty cycle with 15 seconds on and 10 seconds off. The total sonication time was 16 hours. During ultrasonication, ozone gas produced by an oxygen concentrator (OxyMax 8, Longevity Resources) and ozone generator (Ext 120-T, Longevity Resources) was bubbled into the mixture at a flow rate 500 ml/minute to oxidize the surfaces of the carbon nanotubes. After ozone treatment and sonication for 16 hours, 2 grams of PEI (polyethyleneineimine, Mw: 25,000, Sigma-Aldrich) is added to the dispersion and sonicated for another 4 hours under the same conditions to functionalize the oxidized nanotubes. The PEI functionalized nanotube dispersions are then adjusted to a pH of 6 using glacial-acetic acid (Sigma Aldrich) in order to protonate the amine groups and form a stable dispersion of positively charged carbon nanotubes.

To establish the sensing mechanism, carbon nanotube dispersions were used to electrophoretically deposit nanotubes onto a non-woven fabric composed of randomly oriented aramid fibers held together with a binder of cross-linked polyester (20601, 50 g/m^2, Technical Fiber Products). These non-woven fabrics, often referred to as surface veils, are commonly used in advanced fiber reinforced composites for improving the surface finish. The fiber surfaces in a surface veil are designed to be compatible with common polymer

matrix materials and were chosen for their compatibility with CNT-PEI functionality established in our prior research. Using the approach of An *et al.* the non-conductive aramid veil was placed in direct contact with a 316 stainless steel cathode under slight tension with the help of elastic bands to ensure intimate contact with the electrode. A counter electrode of the same stainless steel was placed a fixed distance from the cathode using insulating glass/epoxy composite spacers. The assembly was then immersed in the carbon nanotube dispersion and electrophoretic deposition was carried out under direct current (DC) field strength of 22 V/cm for 8 minutes. The coated aramid fabric is then dried in a convection oven for 15 minutes at 120°C.

For comparison, two other specimens were characterized for their sensing response: (1) specimens were prepared by dip coating the aramid fabric in a commercially-available carbon nanotube sizing and (2) a conductive carbon fiber random mat with random fibers (20301, 50g/m^2 Technical Fiber Products). The sizing specimens were produced by dip coating the aramid veil in an aqueous solution of commercially available carbon nanotube sizing (SIZICYL™ XC R2G, Nanocyl, Belgium). The solution was prepared by mixing 1 part of sizing with 2 parts of ultra-pure water by weight and mixed in a centrifugal mixer (THINKY® ARM-310) at 2000 rpm for 120 seconds and then sonicated for 30 minutes in an ultrasonic bath (Branson® 1510). The aramid veil was dipped in the solution for 10 minutes after which it was flipped and kept for another 10 minutes followed by drying in a convection oven for 15 minutes at 150°C. The carbon fiber veil was used ‘as is’ without any treatment.

Sensor Preparation and Characterization:

All specimens were 100 mm long and 25.4 mm wide. The specimens were laminated in 0.127 mm (5 mils) thick plastic sheets using a heat laminating machine (Saturn 95, Fellowes). For conducting electrical measurements, electrodes and lead wires attached to the specimen using conductive silver paint (SPI supplies) and a 2 part conductive epoxy resin (Epoxies 40–3900) to keep the contact resistance to a minimum. The electrodes were attached at the distance of 6.25 mm from the edge of the specimen. Electrical measurements were made using a voltage current meter (Keithley 6430 Sub Femtoamp Remote Sourcemeter). A constant source voltage was applied to the specimens during the test and the current was measured to calculate the change in resistance. The measurements were synchronized using a customized LabVIEW program.

An electrically actuated load frame (Instron 8562 with a 100 kN load cell) was used for testing specimens to 40 MPa in a load controlled mode. For applying low pressures, Instron MicroTester 5848 with 500 N load cell was used with a displacement rate of 2.54 mm/minute. Scanning Electron Microscopy (SEM) was conducted using an AURIGA™ 60 Crossbeam™ FIB-SEM with an acceleration voltage of 3 kV. The specimens were coated with a thin (~5 nm) conductive layer of Pd/Au to minimize sample charging using a vacuum sputter coater (Denton Desk IV, Denton Vacuum, LLC)

Supplementary Material

Refer to Web version on PubMed Central for supplementary material.

ACKNOWLEDGMENTS

The authors gratefully acknowledge the funding support from Delaware INBRE program, with a grant from the National Institute of General Medical Sciences - NIGMS (P20 GM103446) and the state of Delaware and National Science Foundation (Grant CMMI 1254540: Dr. Mary Toney, Program Director). The authors acknowledge Dr. Yong Zhao for helping with Scanning Electron Microscopy and Stephen Durabano and John Thiravong for helping in the testing of specimens.

REFERENCES

(1). Someya T; Sekitani T; Iba S; Kato Y; Kawaguchi H; Sakurai T A Large Area, Flexible Pressure Sensor Matrix with Organic Field-Effect Transistors for Artificial Skin Applications. Proc. Natl. Acad. Sci. U. S. A 2004, 101 (27), 9966–9970. [PubMed: 15226508]

(2). Jeong JW; Yeo WH; Akhtar A; Norton JJS; Kwack YJ; Li S; Jung SY; Su Y; Lee W; Xia J; et al. Materials and Optimized Designs for Human-Machine Interfaces via Epidermal Electronics. Adv. Mater 2013, 25 (47), 6839–6846. [PubMed: 24327417]

(3). Takei K; Takahashi T; Ho JC; Ko H; Gillies AG; Leu PW; Fearing RS; Javey A Nanowire Active Matrix Circuitry for Low-Voltage Macroscale Artificial Skin. Nat. Mater 2010, 9 (10), 821–826. [PubMed: 20835235]

(4). Gerratt AP; Michaud HO; Lacour SP Elastomeric Electronic Skin for Prosthetic Tactile Sensation. Adv. Funct. Mater 2015, 25 (15), 2287–2295.

(5). Li T; Luo H; Qin L; Wang X; Xiong Z; Ding H; Gu Y; Liu Z; Zhang T Flexible Capacitive Tactile Sensor Based on Micropatterned Dielectric Layer. Small 2016, 12 (36), 5042–5048. [PubMed: 27323288]

(6). Son D; Lee J; Qiao S; Ghaffari R; Kim J; Lee JE; Song C; Kim SJ; Lee DJ; Jun SW; et al. Multifunctional Wearable Devices for Diagnosis and Therapy of Movement Disorders. Nat. Nanotechnol 2014, 9 (5), 397–404. [PubMed: 24681776]

(7). Choi DY; Kim MH; Oh YS; Jung S-H; Jung JH; Sung HJ; Lee HW; Lee HM Highly Stretchable, Hysteresis-Free Ionic Liquid-Based Strain Sensor for Precise Human Motion Monitoring. ACS Appl. Mater. Interfaces 2017, 9 (2), 1770–1780. [PubMed: 27996234]

(8). Mannsfeld SCB; Tee BC-K; Stoltenberg RM; Chen CVH-H; Barman S; Muir BVO; Sokolov AN; Reese C; Bao Z Highly Sensitive Flexible Pressure Sensors with Microstructured Rubber Dielectric Layers. Nat. Mater 2010, 9 (10), 859–864. [PubMed: 20835231]

(9). Lee J; Kwon H; Seo J; Shin S; Koo JH; Pang C; Son S; Kim JH; Jang YH; Kim DE; et al. Conductive Fiber-Based Ultrasensitive Textile Pressure Sensor for Wearable Electronics. Adv. Mater 2015, 27 (15), 2433–2439. [PubMed: 25692572]

(10). Lipomi DJ; Vosgueritchian M; Tee BC-K; Hellstrom SL; Lee J. a; Fox CH; Bao Z Skin-like Pressure and Strain Sensors Based on Transparent Elastic Films of Carbon Nanotubes. Nat. Nanotechnol 2011, 6 (12), 788–792. [PubMed: 22020121]

(11). Wang J; Jiu J; Nogi M; Sugahara T; Nagao S; Koga H; He P; Suganuma K A Highly Sensitive and Flexible Pressure Sensor with Electrodes and Elastomeric Interlayer Containing Silver Nanowires. Nanoscale 2015, 7 (7), 2926–2932. [PubMed: 25588044]

(12). Mandal D; Yoon S; Kim KJ Origin of Piezoelectricity in an Electrospun Poly(vinylidene Fluoride-Trifluoroethylene) Nanofiber Web-Based Nanogenerator and Nano-Pressure Sensor. Macromol. Rapid Commun. 2011, 32 (11), 831–837. [PubMed: 21500300]

(13). Zang Y; Zhang F; Huang D; Gao X; Di C; Zhu D Flexible Suspended Gate Organic Thin-Film Transistors for Ultra Sensitive Pressure Detection. Nat. Commun 2015, 6, 6269. [PubMed: 25872157]

(14). Yang Y; Zhang H; Lin ZH; Zhou YS; Jing Q; Su Y; Yang J; Chen J; Hu C; Wang ZL Human Skin Based Triboelectric Nanogenerators for Harvesting Biomechanical Energy and as Self-Powered Active Tactile Sensor System. ACS Nano 2013, 7 (10), 9213–9222. [PubMed: 24006962]

(15). Yao H. Bin; Ge J; Wang CF; Wang X; Hu W; Zheng ZJ; Ni Y; Yu SH A Flexible and Highly Pressure-Sensitive Graphene Polyurethane Sponge Based on Fractured Microstructure Design. Adv. Mater 2013, 25 (46), 6692–6698. [PubMed: 24027108]

(16). Pan L; Chortos A; Yu G; Wang Y; Isaacson S; Allen R; Shi Y; Dauskardt R; Bao Z An Ultra-Sensitive Resistive Pressure Sensor Based on Hollow Sphere Microstructure Induced Elasticity in Conducting Polymer Film. Nat. Commun 2014, 5, 1–8.

(17). Gong S; Schwalb W; Wang Y; Chen Y; Tang Y; Si J; Shirinzadeh B; Cheng W A Wearable and Highly Sensitive Pressure Sensor with Ultrathin Gold Nanowires. Nat. Commun 2014, 5, 1–8.

(18). Liao X; Liao Q; Zhang Z; Yan X; Liang Q; Wang Q; Li M; Zhang Y A Highly Stretchable ZnO@Fiber-Based Multifunctional Nanosensor for Strain/Temperature/UV Detection. Adv. Funct. Mater 2016, 26 (18), 3074–3081.

(19). Wu W; Wen X; Wang ZL Taxel-Addressable Matrix of Vertical-Nanowire Piezotronic Transistors for Active and Adaptive Tactile Imaging. 2013, 340, 952–957.

(20). Lai YC; Ye BW; Lu CF; Chen CT; Jao MH; Su WF; Hung WY; Lin TY; Chen YF Extraordinarily Sensitive and Low-Voltage Operational Cloth-Based Electronic Skin for Wearable Sensing and Multifunctional Integration Uses: A Tactile-Induced Insulating-to-Conducting Transition. Adv. Funct. Mater 2016, 26 (8), 1286–1295.

(21). Ge J; Sun L; Zhang FR; Zhang Y; Shi LA; Zhao HY; Zhu HW; Jiang HL; Yu SH A Stretchable Electronic Fabric Artificial Skin with Pressure-, Lateral Strain-, and Flexion-Sensitive Properties. Adv. Mater 2016, 28 (4), 722–728. [PubMed: 26618615]

(22). Tung TT; Nine MJ; Krebsz M; Pasinszki T; Coghlan CJ; Tran DNH; Losic D Recent Advances in Sensing Applications of Graphene Assemblies and Their Composites. Adv. Funct. Mater 2017, Article 1702891.

(23). Maheshwari V; Saraf RF High-Resolution Thin-Film Device to Sense Texture by Touch. Science. 2006, 312 (5779), 1501–1504. [PubMed: 16763143]

(24). Lee J; Kim S; Lee J; Yang D; Park BC; Ryu S; Park I A Stretchable Strain Sensor Based on a Metal Nanoparticle Thin Film for Human Motion Detection. Nanoscale 2014, 6 (20), 11932–11939. [PubMed: 25175360]

(25). Jung T; Yang S Highly Stable Liquid Metal-Based Pressure Sensor Integrated with a Microfluidic Channel. Sensors 2015, 15 (5), 11823–11835. [PubMed: 26007732]

(26). Wu C-Y; Liao W-H; Tung Y-C Integrated Ionic Liquid-Based Electrofluidic Circuits for Pressure Sensing within Polydimethylsiloxane Microfluidic Systems. Lab Chip 2011, 11 (10), 1740–1746. [PubMed: 21451820]

(27). Stampfer RC; Helbling T; Obergfell D; Schöberle B; Tripp MK; Jungen A; Roth S; Bright VM; Hierold C Fabrication of Single-Walled Carbon-Nanotube-Based Pressure Sensors. Nano Lett. 2006, 6 (2), 233–237. [PubMed: 16464041]

(28). Hwang J; Jang J; Hong K; Kim KN; Han JH; Shin K; Park CE Poly(3-Hexylthiophene) Wrapped Carbon Nanotube/poly(dimethylsiloxane) Composites for Use in Finger-Sensing Piezoresistive Pressure Sensors. Carbon N. Y 2011, 49 (1), 106–110.

(29). Kim SY; Park S; Park HW; Park DH; Jeong Y Highly Sensitive and Multimodal All-Carbon Skin Sensors Capable of Simultaneously Detecting Tactile and Biological Stimuli. Adv. Mater 2015, 27 (28), 4178–4185. [PubMed: 26095173]

(30). Wu X; Han Y; Zhang X; Zhou Z; Lu C Large-Area Compliant, Low-Cost, and Versatile Pressure-Sensing Platform Based on Microcrack-Designed Carbon Black@Polyurethane Sponge for Human–Machine Interfacing. Adv. Funct. Mater 2016, 26 (34), 6246–6256.

(31). Choong CL; Shim MB; Lee BS; Jeon S; Ko DS; Kang TH; Bae J; Lee SH; Byun KE; Im J; et al. Highly Stretchable Resistive Pressure Sensors Using a Conductive Elastomeric Composite on a Micropyramid Array. Adv. Mater 2014, 26 (21), 3451–3458. [PubMed: 24536023]

(32). Pang C; Lee G-Y; Kim T; Kim SM; Kim HN; Ahn S-H; Suh K-Y A Flexible and Highly Sensitive Strain-Gauge Sensor Using Reversible Interlocking of Nanofibres. Nat. Mater 2012, 11 (9), 795–801. [PubMed: 22842511]

(33). Tian H; Shu Y; Wang X-F; Mohammad MA; Bie Z; Xie Q-Y; Li C; Mi W-T; Yang Y; Ren T-L A Graphene-Based Resistive Pressure Sensor with Record High-Sensitivity in a Wide Pressure Range. Sci. Rep 2015, 5 (1), 8603. [PubMed: 25721159]

(34). Jung S; Kim JH; Kim J; Choi S; Lee J; Park I; Hyeon T; Kim DH Reverse-Micelle-Induced Porous Pressure-Sensitive Rubber for Wearable Human-Machine Interfaces. Adv. Mater 2014, 26 (28), 4825–4830. [PubMed: 24827418]

(35). Falvo MR; Clary GJ; Taylor RM; Chi V; Brooks FP; Washburn S; Superfine R Bending and Buckling of Carbon Nanotubes under Large Strain. Nature 1997, 389 (6651), 582–584. [PubMed: 9335495]

(36). Sazonova V; Yaish Y; Üstünel H; Roundy D; Arias TA; McEuen PL A Tunable Carbon Nanotube Electromechanical Oscillator. Nature 2004, 431 (7006), 284–287. [PubMed: 15372026]

(37). Qian D; Wagner GJ; Liu WK; Yu MF; Ruoff RS Mechanics of Carbon Nanotubes. Appl. Mech. Rev 2002, 55 (6), 495–533.

(38). Yakobson BI; Brabec CJ; Bernholc J Nanomechanics of Carbon Tubes: Instabilities beyond Linear Response. Phys. Rev. Lett 1996, 76 (14), 2511–2514. [PubMed: 10060718]

(39). Lourie O; Cox D; Wagner H Buckling and Collapse of Embedded Carbon Nanotubes. Phys. Rev. Lett 1998, 81 (8), 1638–1641.

(40). An Q; Rider AN; Thostenson ET Electrophoretic Deposition of Carbon Nanotubes onto Carbon-Fiber Fabric for Production of Carbon/epoxy Composites with Improved Mechanical Properties. Carbon N. Y 2012, 50, 4130–4143.

(41). An Q; Rider AN; Thostenson ET Hierarchical Composite Structures Prepared by Electrophoretic Deposition of Carbon Nanotubes onto Glass Fibers. ACS Appl. Mater. Interfaces 2013, 5 (6) 2022–2032. [PubMed: 23379418]

(42). Rider AN; An Q; Brack N; Thostenson ET Polymer Nanocomposite - Fiber Model Interphases: Influence of Processing and Interface Chemistry on Mechanical Performance. Chem. Eng. J 2015, 269, 121–134.

(43). Naito K; Tanaka Y; Yang JM; Kagawa Y Tensile Properties of Ultrahigh Strength PAN-Based, Ultrahigh Modulus Pitch-Based and High Ductility Pitch-Based Carbon Fibers. Carbon N. Y 2008, 46 (2), 189–195.

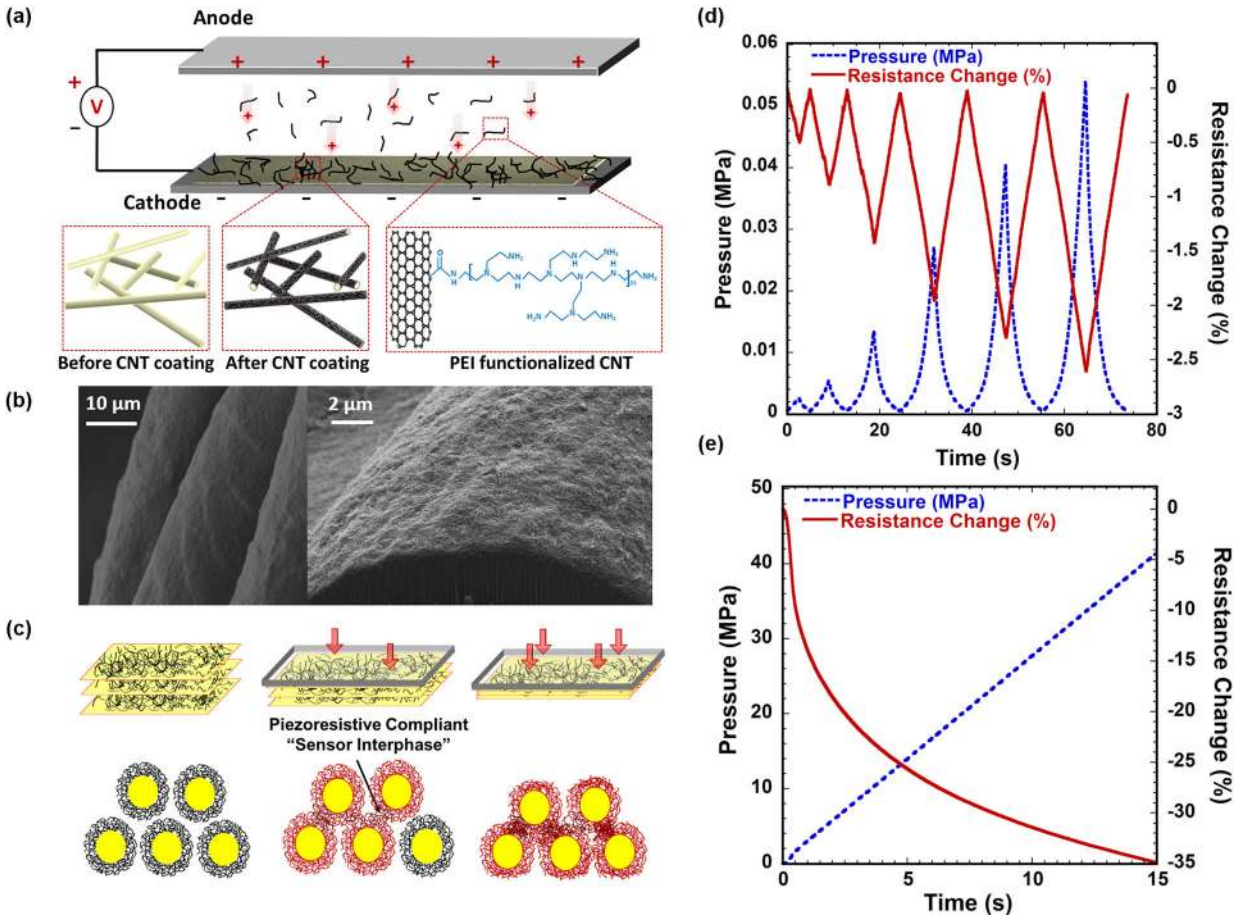

Figure 1.

a) A schematic illustration of the EPD process to deposit PEI-CNT on a non-woven aramid veil. b) SEM micrographs of PEI-CNT deposited on wool fibers showing their scale-like cuticle structure (left) and a cross-section of an aramid fiber showing a uniform thickness, porous nanocomposite layer of PEI-CNT (right). c) A schematic representation of PEI-CNT coated aramid veil under applied pressure showing the proposed sensing mechanism. d) Resistance response of EPD PEI-CNT sensor subjected to low pressures in the tactile and object manipulation range. e) Resistance response of the sensor under an extremely wide range of pressure sensing from 0 to 40 MPa.

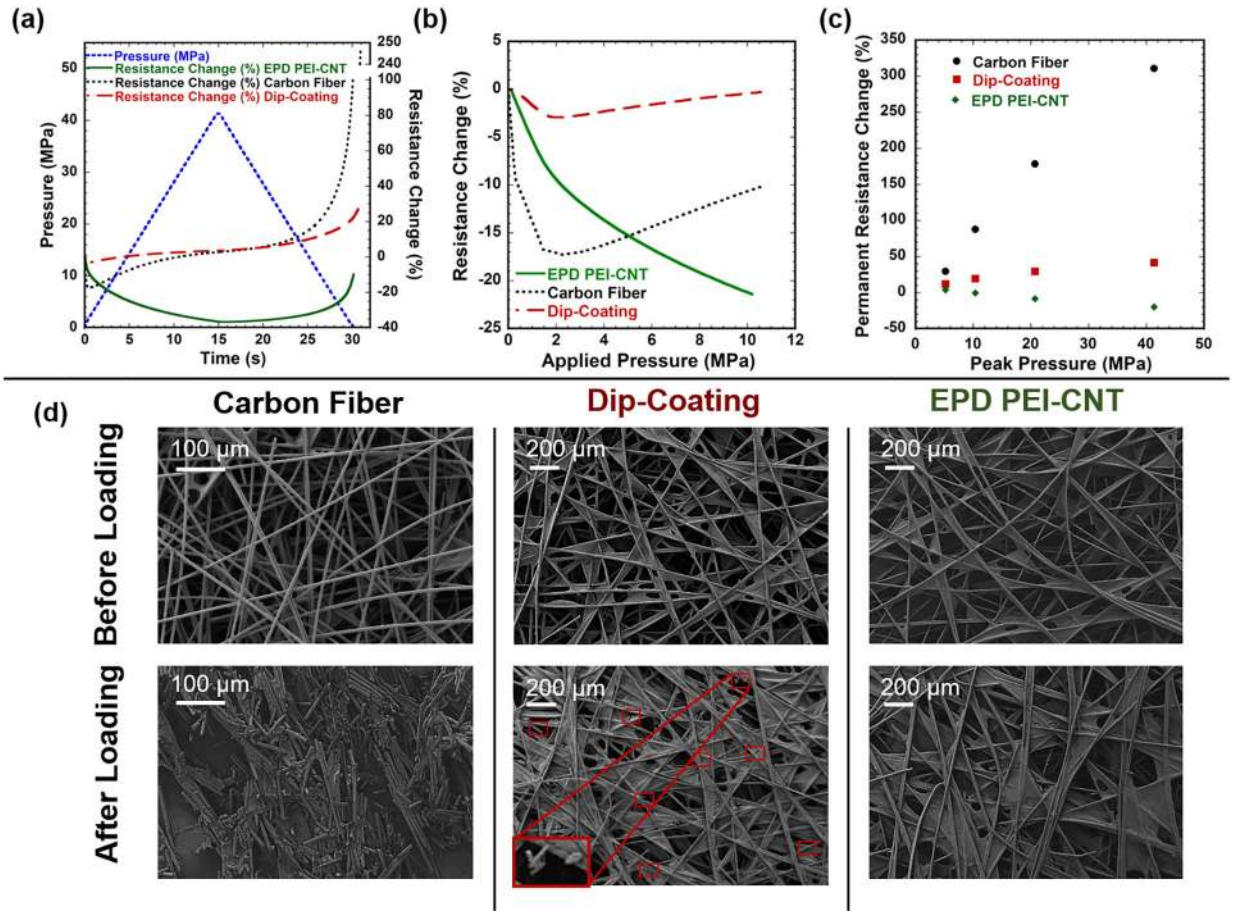

Figure 2.

a) Resistance response of EPD PEI-CNT, carbon fiber, and dip-coating sensors when subjected to a pressure of 40 MPa. b) Expanded view of the resistance response of the sensors at low pressures highlighting the increase in resistance for carbon fiber and dip-coating sensors due to damage. c) Permanent increase in resistance for carbon fiber and dip-coating sensor indicating increasing damage with increasing peak loads as compared to decreasing resistance for EPD PEI-CNT sensors. d) SEM micrographs of the sensors before and after loading to 40 MPa. Broken fibers in carbon fiber sensors and small debris in dip-coating specimen is visible whereas the EPD PEI-CNT sensors show no significant damage.

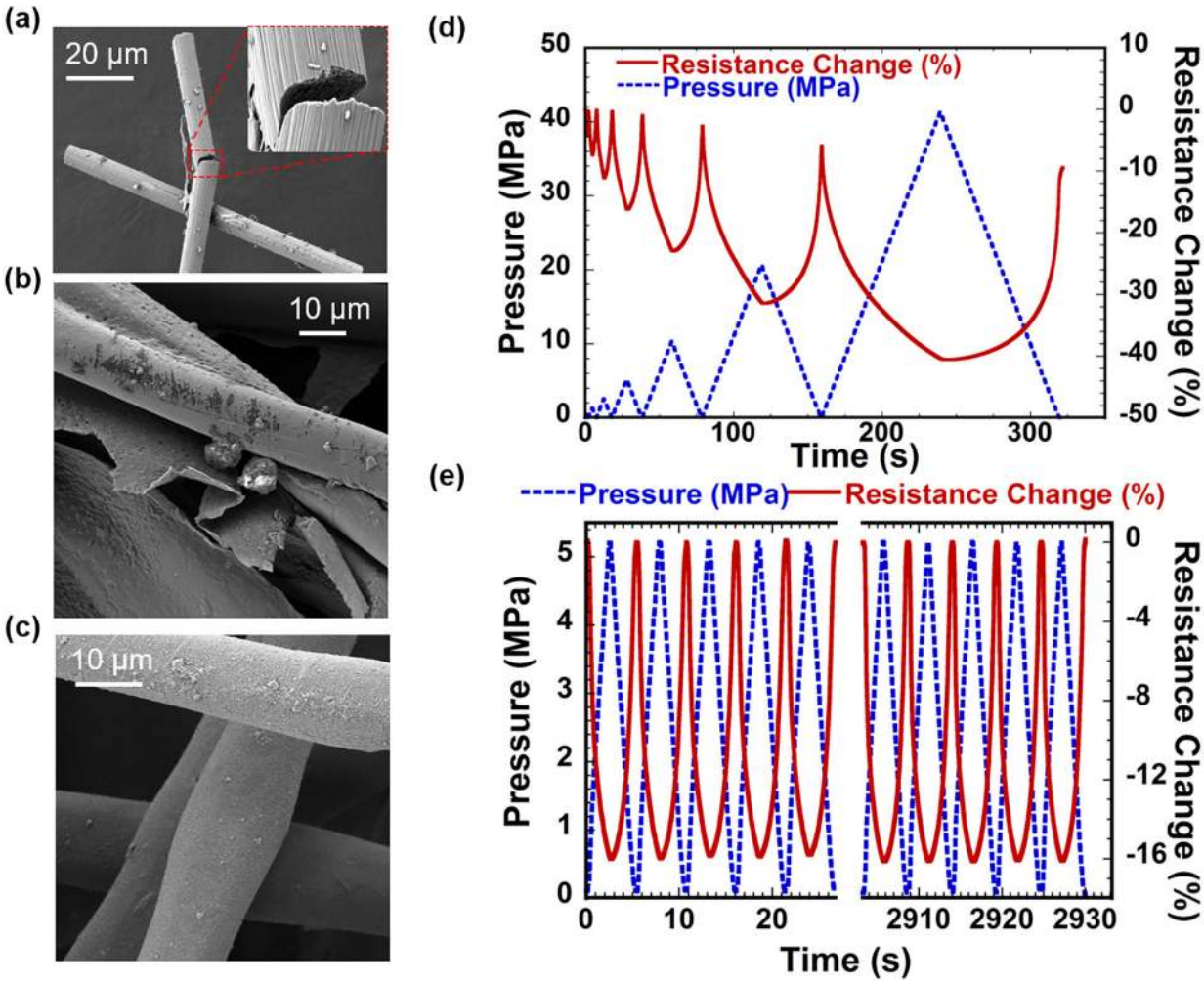

Figure 3.

Scanning electron micrographs after loading to 40MPa of a) Carbon fiber sensor b) Dip-coating sensor showing damage to carbon nanotube coating and c) EPD PEI-CNT sensor bulging of fibers but no evident damage. d) Resistance response to progressively increasing cyclic loading of EPD PEI-CNT sensor. e) 1st five and last five cycles of EPD PEI-CNT sensor when subjected to a 550 cycle test. The resistance response is highly repeatable due to the robustness of the PEI-CNT nanocomposite coating in the EPD PEI-CNT sensor.

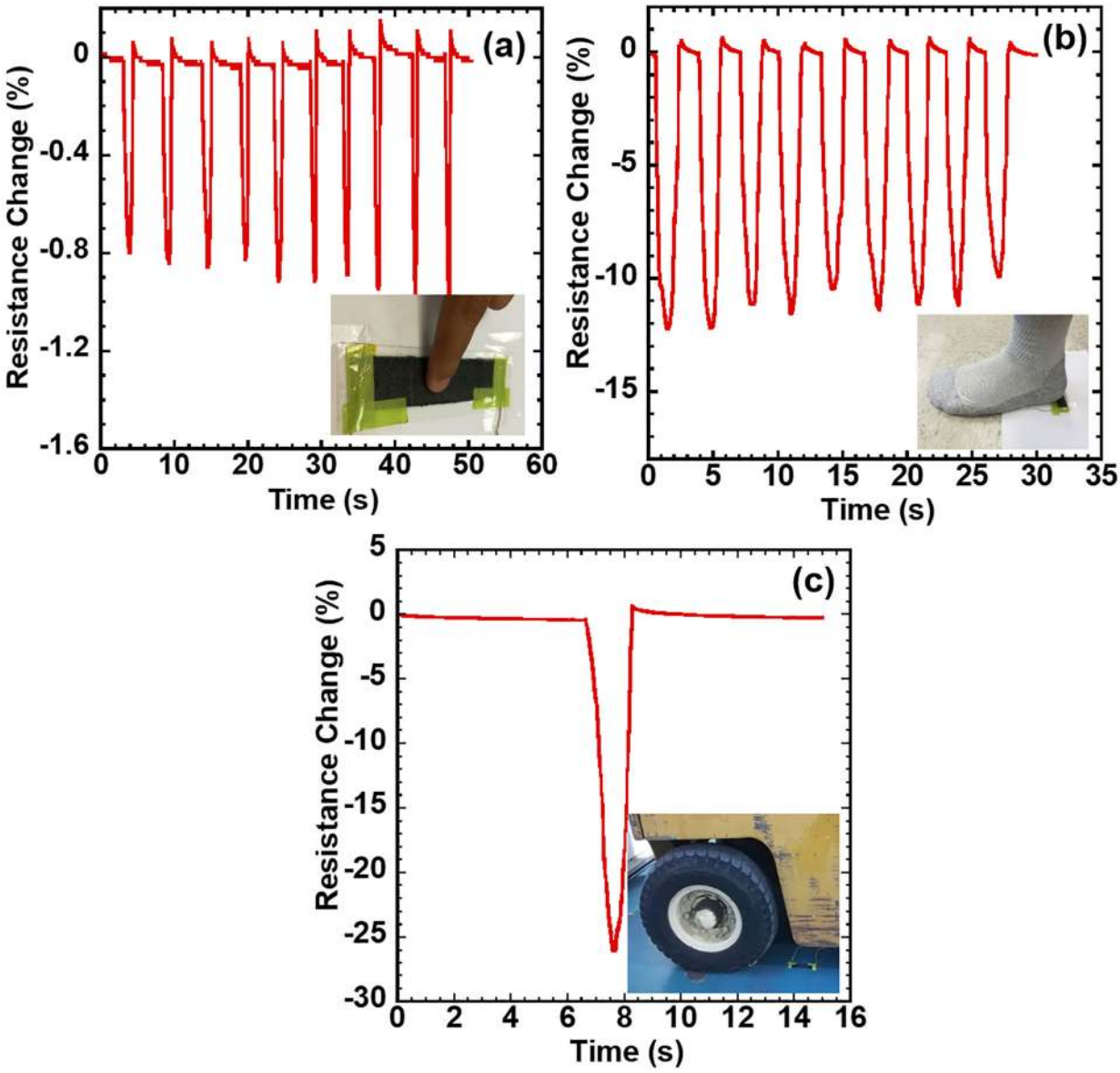

Figure 4.

Resistance response of the sensor when subjected to a) tactile pressures applied by finger tapping, b) body weight pressures applied by standing on the sensor and c) extremely high pressures applied by driving a forklift over the sensor.